Available online at www.sciencedirect.com

ScienceDirect

Procedia Engineering 81 (2014) 1342 – 1347

Procedia Engineering

www.elsevier.com/locate/procedia

11th International Conference on Technology of Plasticity, ICTP 2014, 19-24 October 2014, Nagoya Congress Center, Nagoya, Japan

Plane strain compression test and simple shear test of single crystal pure iron

Shintaro Yabe*, Motoki Terano, Masahiko Yoshino

Department of Mechanical and Aerospace, Tokyo Institute of Technology, 2-12-1, Ookayama, Meguro-ku, Tokyo, 152-8552, Japan

Abstract

Material tests of single crystal pure iron are reported in this paper. Four kinds of specimens with various crystal orientations were cut out from a single crystal rod by WEDM. These specimens were subjected to plane strain compression tests and simple shear tests. Stress-strain relationships were obtained from the load-stroke curves measured in these material tests. These results showed that the stress-strain relationship depends strongly on the crystal orientation. Effects of the crystal orientation on the stress-strain relationship were discussed by the comparison with calculation based on the crystalline plasticity theory. In addition, plastic deformation of single crystal specimens by the material tests was studied by using Electron Back Scattering Diffraction (EBSD) analysis.

Selection and peer-review under responsibility of the Department of Materials Science and Engineering, Nagoya University

Keywords; Single crystal pure iron; Crystal orientation; Electron Backscatter Diffraction(EBSD)

1. Introduction

In recent years, developments of high performance materials are demanded in order to address recent global problems, such as energy problems, natural resource problems and environmental problems. Although alloying is an effective method to develop new materials, it is not preferable in terms of the natural resource conservation and the recycle. In the meantime, a microstructure control by Thermo-Mechanical Control Process (TMCP) is much

* Corresponding author. Tel.: +81-3-5734-2640; fax: +81-3-5734-2811.
E-mail address: yabe.s.aa@m.titech.ac.jp

Selection and peer-review under responsibility of the Department of Materials Science and Engineering, Nagoya University
doi:10.1016/j.proeng.2014.10.154

advantageous for material developments because TMCP does not need additive elements. In fact, many high performance steels, such as ultrafine grained steels, magnetic steel sheets, were developed by TMCP.

Many researches about the microstructure control by TMCP have been conducted for long years [1, 2, 3]. However, most of them studied microstructure changes from the statistical point of view using polycrystalline specimens, in which uncertainty of initial crystalline structure cannot be avoided. Thus, in spite of their endeavors, they still need enormous amount of experimental trials in order to develop a new TMCP method. Since the recrystallization is the primary process that governs microstructure changes in TMCP, it is important to study effects of the plastic deformation of each crystal grain on recrystallization in order to advance TMCP technology. However, plastic deformation characteristics of a single crystal grain have not been revealed yet.

In this paper, stress-strain relationships of a single crystal iron are studied by means of plain strain compression tests and simple shear tests. In addition, effects on crystal orientation of before and after material tests were analyzed by using Electron Backscatter Diffraction (EBSD).

Nomenclature

$\boldsymbol{R}$	crystal orientation tensor
k	the number of the slip system
τ^k	stress vector acting on the k th slip plane $\boldsymbol{b}^k$ unit slip vector on the k th slip system, which is parallel to Burger's vector
$\boldsymbol{n}^k$	normal vector of the slip plane that the k th slip system exists
$\boldsymbol{\sigma}$	stress tensor applied to a specimen

2. Plane strain compression test

2.1. Experimental procedure

Specimens were cut out from a single crystal pure iron rod, which is 5 mm in diameter and 50 mm in length, by using a Wire Electric Discharge Machine (WEDM). Dimensions of specimens were 3 mm in width and 0.7 mm in thickness as shown in Fig. 1. Four types of specimens with various crystal orientations were made. Their crystal orientations are listed in Table 1. *l*-*w*-*t* in the table indicates the coordinate system presented in Fig.1; *t* indicates the axial direction of the single crystal rod, *l* indicates longitudinal direction of the specimen, and *w* indicates transverse direction. Specimens A and B were cut out from a single crystal rod whose axial crystal orientation was <100>. Specimen C and D were cut out from a single crystal rod whose axial crystal orientation was <111>.

Specially designed material test jigs were developed for the plane strain compression tests and for simple shear tests. Fig. 2 is the schematic illustration of the plane strain compression test. As for the plane strain compression test jig, the width of upper and lower punches was the 3.0 mm. The thickness was designed to be equal to the width of specimens in order to maintain plane strain deformation of a specimen. As shown by the Fig. 2(a), the constraint plates were placed on both the front side and the back side of the punches. The specimen is placed between the punches and the constraint plates. When the upper punch is pushed down during the material test, the specimen is extended to horizontal directions. Since deformation to *w* direction is restricted by the constraint plates, strain to *w* direction is kept zero. As a result, the specimen is tested under plane strain condition. In the experiment, the punch speed was 0.002 mm/s. In the material test, the deformation load and variation in thickness were measured. In order to reduce friction, the testing jig and specimens were lubricated by molybdenum disulfide paste. After the material tests, the specimen was cut on the center line of the specimen along *t*-*l* plane by using WEDM. Then the cross-section of the specimen was polished by using colloidal silica, and was subjected to crystal orientation analysis by using EBSD.

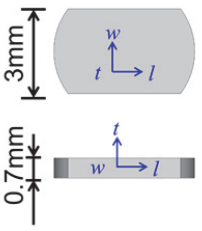

Table 1. Crystal orientation of spcimens.

	l - w - t
A	<100>-<100>-<100>
B	<110>-<110>-<100>
C	<110>-<112>-<111>
D	<112>-<110>-<111>

Fig. 1. Dimensions of specimens.

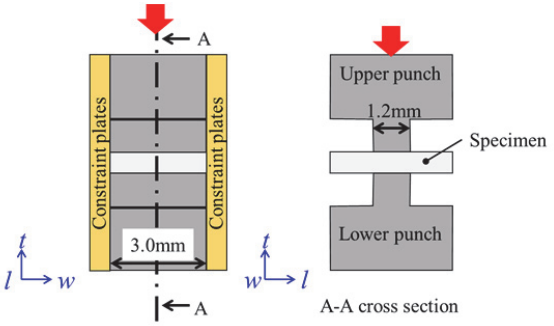

(a) Side view (b) Front view

Fig. 2. Plane strain compression test.

2.2. Result and discussion

Fig. 3 shows the load-stroke curves obtained from the plane strain compression tests. It is found that the load-stroke curves depend on crystal orientation of the specimen. These load-stroke curves were converted to apparent compressive stress-strain under plane strain condition. Fig. 4 shows the apparent stress-strain curves of each specimen.

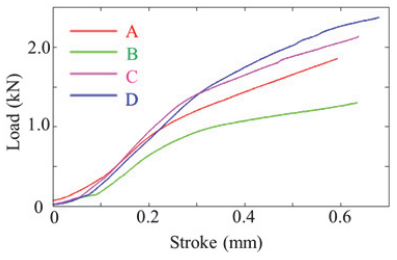

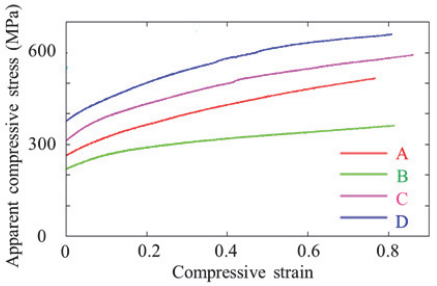

Fig. 3. Load – stroke curves for plane strain compression test. Fig. 4. Stress–strain curves obtained from plane strain compression test.

In order for the comparison with experimental results and the crystal plasticity theory, the resolved shear stresses working on the k th slip systems, whose unit slip vector is $\mathbf{b}^{\mathbf{k}}$ and normal vector of the slip plane is $\mathbf{n}^{\mathbf{k}}$, were calculated by eq.(1) [4]. $\boldsymbol{\sigma}$ is the stress tensor applied to a specimen and $\mathbf{R}$ is a crystal orientation tensor.

$$\boldsymbol{\tau}^{\mathbf{k}} = \mathbf{R}\,\mathbf{b}^{\mathbf{k}} \bullet \boldsymbol{\sigma} \bullet \mathbf{n}^{\mathbf{k}\,\mathbf{T}}\mathbf{R}^{\mathbf{T}}, \tag{1}$$

where τ^k is the resolved shear stresses acting on the k th slip system. In this calculation, twelve primary slip systems in an iron crystal lattice (bcc) were taken into account. The resolved shear stresses on the all of slip systems were calculated by Eq. (1), and maximum shear stress $\tau_{\max}$ is determined. By comparing $\tau_{\max}$ of four specimens of different crystal orientations, effects of crystal orientation on the apparent compression stress were estimated. Table 2 compares the magnitude relation of the compression stress of the specimens obtained from the experiments (Fig. 4) and calculated from compression stress.

It is found that magnitude relation of specimen of A, C, D agree with that of the theoretical estimation. However, the apparent stress of B is the smallest in the experimental data, but that of theory is greater than stress of C. It is attributed to the instable deformation of specimens. Fig.5 shows an example of a specimen. It is apparently distorted into axisymmetric shape. This is due to effects of friction between the specimen and the punch/die, and

anisotropy of a single crystal material. In order to clarify effects of crystal orientation, it is necessary to compare deformation stresses by utilizing Crystal Plasticity Finite Element (CP-FEM) simulations.

Table 2. Comparison of results and estimation about compressive stress magnitude correlation.

Experimental result	Theoretical estimation
B < A < C < D	A < C < B < D

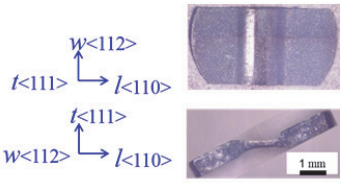

Fig. 5. Example of the compressed specimen (specimen C) Upper picture is the top view and lower one is the side view.

Fig. 6 shows the result of EBSD analysis on the specimen C. Compressed zone of the specimen is observed. The inverse pole figure map indicates crystal orientation observed from *t* direction by the color of the standard triangle of the inset. It is found that crystal orientation in the compressed area is almost <111>. This indicates that crystal orientation did not change by the plane strain compression test. It is also found from the inverse pole figure map and the Image Quality (IQ) map that shear deformation occurred on shear planes inclined to 30~35 degrees from *l* direction. However, this shear deformation did not cause crystal rotation as seen in the inverse pole figure map.

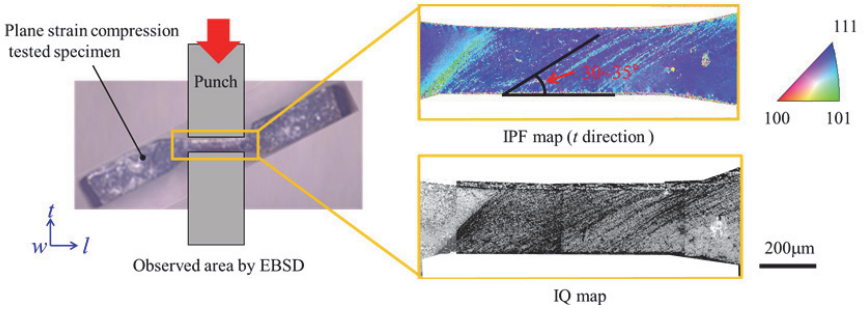

Fig. 6. Inverse pole figure map and IQ map for plane strain compression test (specimen C).

3. Simple shear test

3.1. Experimental procedure

Fig. 7 illustrates the testing jig used for the simple shear tests. The width of punch was 1.8 mm and shearing clearances were 0.1 mm in both sides of the punch edges. After setting the specimens on the die, the punch was pushed down at the speed of 0.002 mm/s. In this procedure, applied load was measured. To reduce friction between the testing jig and a specimen, the specimen was lubricated by molybdenum disulfide paste.

After the shearing test, crystal orientation of the specimen was analyzed using EBSD. For the EBSD analysis on the cross section of the *t*-*l* plane, specimens were cut along *t*-*l* plane by using WEDM, and polished with colloidal silica slurry.

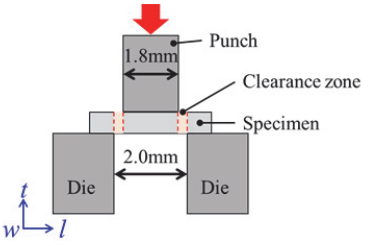

Fig. 7. Simple shear test.

3.2. Result and discussion

Fig. 8 shows load-stroke curves of specimens of various crystal orientations obtained from the simple shear tests. These data were converted to apparent shear stress, which is average shear stress acting on the shear zone of the specimen. Fig. 9 shows variation of apparent shearing stress against apparent shearing strain. It is confirmed that shear stress depends on crystal orientation. However, trend of the stress variation is not very apparent when compared to the data of plan strain compressive test (Fig. 4).

The resolved shear stresses on the all of slip systems were also calculated for the shearing tests by the same calculation as the plane strain compressive tests. Then, the maximum shear stress τ_{max} was determined, and effects of crystal orientation on the apparent shear stress were estimated. Table 3 compares the magnitude relation of the shear stresses of the specimens obtained from the experiments (Fig. 9) and calculated shear stress. The magnitude relation of the experimental result does not agree with that of theoretical estimation.

This is attributed to deformation of specimens. Fig. 10 shows pictures of a specimen after the shear test. It is found that the specimen was sheared near the edges of the punch/die. However at the same time, the specimen was curved by the shear test, which caused bending deformation in the specimen. In the theoretical estimation, it was difficult to take into account of the effects of bending.

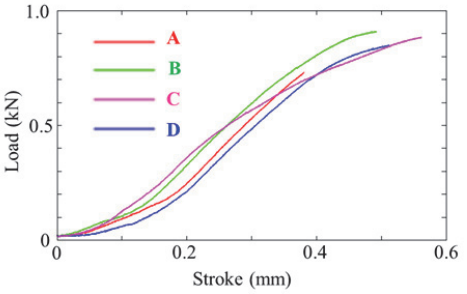

Fig.8. Load – stroke curves for simple shear tests.

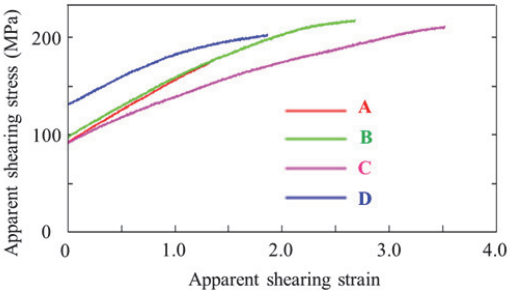

Fig. 9. Stress – strain curves for simple shear tests.

Table 3. Comparison of results and estimation about shearing stress magnitude correlation.

Experimental result	Theoretical estimation
C < A < B < D	D < C < B < A

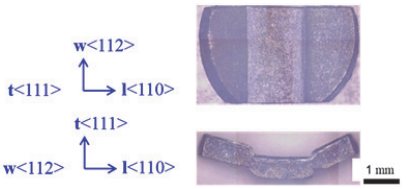

Fig. 10. Geometry of one of the sheared specimen.

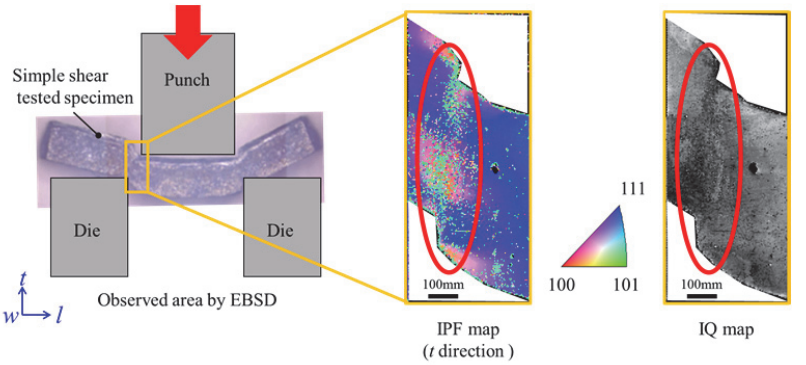

Fig. 11. Inverse pole figure map and IQ map for the simple shear test.

Fig. 11 shows inverse pole figure map and IQ map on the cross section of a tested specimen. The inverse pole figure map shows crystal orientation observed from t direction by the colour of the standard triangle. Complicated distribution of crystal orientation is observed in the inverse pole figure map. IQ map also indicates that lattice distortion is not uniform in the area indicated by circles in Fig. 11. Although simple shear deformation was applied to the specimen, complicated strain distribution arose. One of the reasons is the bending deformation of the specimen. Another is stress concentration at the edge of the punch and the die. It is necessary to improve experimental technique to get accurate stress-strain relationship on the shear test. In addition, comparison with numerical simulation by CP-FEM is useful to reveal fundamental deformation characteristics of a single crystal material in the future study.

4. Conclusions

(1) Plane strain compression tests and simple shear tests were conducted on the single crystal pure iron specimens with four kinds of different crystal orientations. Effect of crystal orientation on magnitude relation of stress-strain curves was discussed.
(2) Stress-strain curves obtained from the plane strain compression tests showed almost the same trend with the theoretical compressive stress estimated by crystalline plasticity theory. However, stress-strain curves obtained from the simple shear tests did not agree to the theoretical estimation. The difference was attributed to the axisymmetric deformation of a specimen, the bending deformation of the specimen, and the complicated strain distribution in the deformation zone.
(3) Distributions of crystal orientations in the tested specimens were analyzed by using Electron Backscatter Diffraction (EBSD). It was revealed that crystal rotation did not occur in the plane strain compression tests, but shear deformation occurred along with shear plane inclined to the 30~35 degrees from l direction.
(4) On the other hand, the simple shear tests occurred complicated strain distribution in a specimen, which could not be taken into account in the theoretical model. Improvements of the experimental technique and CP-FEM simulation were necessary in the future study.

Acknowledgements

This work was funded by THE AMADA FOUNDATION, AF-2011013.

References

[1]A., I., Fernan, Z., P., Uranga, B., Lopez, and J., M., Rodriguez-Ibabe, 2000. Static Recrystallization Behaviour of a Wide Range of Austenite Grain Sizes in Microalloyed Steels. In: ISIJ International, 40, 9, 893-901.
[2]Hirota, N.,Yin, F.,Inoue, T.,Azuma, T., 2008. Recrystallization and Grain Growth Behavior in Severe Cold-rolling Deformed SUS316L Steel under Anisothermal Annealing Condition. In: ISIJ International, 48, 4, 475-482 .
[3]Omura, T.,Hayakawa, Y.,2013. Influence of Primary-Recrystallization Texture on Selective Growth of Goss Grains. In: Materials Transactions, 54, 1, 14 – 21.
[4]Roters, F., Eisenlohr, P., Hantcherli, L., Tjahjanto, D.D., Bieler, T.R., Raabe, D., 2010. Overview of constitutive laws, kinematics, homogenization and multiscale methods in crystal plasticity finite-element modeling: Theory, experiments, applications. 58, 4, 1152–1211.